

Borrelia burgdorferi Co-Localizing with Amyloid Markers in Alzheimer's Disease Brain Tissues

Alireza G. Senejani^{a,*}, Jasmin Maghsoudlou^a, Dina El-Zohiry^a, Gauri Gaur^a, Keith Wawrzeniak^a, Cristina Caravaglia^a, Vishwa A. Khatri^a, Alan MacDonald^b and Eva Sapi^a

^aDepartment of Biology and Environmental Sciences, University of New Haven, West Haven, CT, USA

^bMolecular Interrogation Research Laboratory, Naples, FL, USA

Accepted 24 October 2021

Pre-press 5 December 2021

Abstract.

Background: Infections by bacterial or viral agents have been hypothesized to influence the etiology of neurodegenerative diseases.

Objective: This study examined the potential presence of *Borrelia burgdorferi* spirochete, the causative agent of Lyme disease, in brain autopsy tissue of patients diagnosed with either Alzheimer's (AD) or Parkinson's diseases.

Methods: Brain tissue sections from patients with age-matched controls were evaluated for antigen and DNA presence of *B. burgdorferi* using various methods. Positive *Borrelia* structures were evaluated for co-localization with biofilm and AD markers such as amyloid and phospho-tau (p-Tau) using immunohistochemical methods.

Results: The results showed the presence of *B. burgdorferi* antigen and DNA in patients with AD pathology and among those, one of them was previously diagnosed with Lyme disease. Interestingly, a significant number of *Borrelia*-positive aggregates with a known biofilm marker, alginate, were found along with the spirochetal structures. Our immunohistochemical data also showed that *Borrelia*-positive aggregates co-localized with amyloid and phospho-tau markers. To further prove the potential relationship of *B. burgdorferi* and amyloids, we infected two mammalian cell lines with *B. burgdorferi* which resulted in a significant increase in the expression of amyloid- β and p-Tau proteins in both cells lines post-infection.

Conclusion: These results indicate that *B. burgdorferi* can be found in AD brain tissues, not just in spirochete but a known antibiotics resistant biofilm form, and its co-localized amyloid markers. In summary, this study provides evidence for a likely association between *B. burgdorferi* infections and biofilm formation, AD pathology, and chronic neurodegenerative diseases.

Keywords: Alzheimer's disease, amyloid, biofilm, Lyme neuroborreliosis, tau proteins

INTRODUCTION

Lyme Borreliosis is a tick-borne multi-systemic illness caused by the spirochete *Borrelia burgdorferi* sensu lato [1–3]. *B. burgdorferi* is known to be neurotropic and can exist in the central nervous

system (CNS) for lengthy periods of time leading to destructive symptomatic neurological disease [4–6], in addition to other clinical manifestations such as a bull's eye rash, flu-like symptoms, arthritis, carditis, and myalgia [7, 8]. Neurological Lyme Borreliosis can manifest as meningitis, cognitive impairment, fatigue, and encephalopathy and can result in brain atrophy, amyloid deposition, and slow progressive dementia [9–15]. These neurological symptoms could persist in patients even post antibiotic treatment [14]. The reoccurrence of Lyme

*Correspondence to: Alireza G. Senejani, Department of Biology and Environmental Sciences, University of New Haven, 300 Boston Post Road, West Haven, CT, 06516, USA. E-mail: asenejani@newhaven.edu.

Borreliosis coupled with antibiotic resistance has been suggested to be due to the formation of different morphological forms of *B. burgdorferi* such as round bodies [16–20]. In the past few years, however, *B. burgdorferi* sensu lato and stricto strains have also demonstrated the capacity to exist in an alternative form called biofilms *in vivo* and *in vitro* [21–23]. Biofilms are complex aggregates of the bacteria that are particularly difficult to eliminate as they have as much as 1000-fold greater antibiotic resistance than the free-living cells [24]. *In vitro* studies have recently shown that *B. burgdorferi* biofilms also exhibit very high degrees of resistance to various antibiotics [25, 26]. Furthermore, a previous clinical study demonstrated the presence of *B. burgdorferi* spirochetes and biofilms along with inflammatory markers in several organs such as skin, brain, heart, kidney, and liver autopsy tissues of a Lyme disease patient who exhibited diverse neurological symptoms and has been treated over a course of 16 years [27].

The connection between *B. burgdorferi* infection and neurodegenerative diseases is suggested previously by several studies [28–36], along with other potential infections such as Herpes viruses, *Chlamydia pneumoniae*, and gingivitis caused by bacteria such as *Porphyromonas gingivalis* as well as *Propionibacterium* and *Helicobacter pylori* [37–45]. However, the infectious origin of Alzheimer's disease (AD) remains to be adequately explored.

In AD, the loss of neurons proceeds in parallel with progression of clinical cognitive impairments [46]. Cerebral neuronal death and compromise of neural networks are accompanied by a loss of brain mass. Amyloid- β (A β) parenchymal deposits and phospho-tau (p-Tau) deposits inside neurons labelled for death are hallmarks of AD [46].

The working hypothesis of this study is that *B. burgdorferi* can be found in brain tissues derived from patients with neurodegenerative diseases and its presence can affect disease progression. The presence of *B. burgdorferi* in autopsy brain tissues of patients from brain bank with well characterized AD and Parkinson's disease were also examined using human hippocampal brain autopsy sections derived from 10 patients with neurodegenerative diseases, along with brain autopsy tissues obtained from a documented case of concurrent Lyme neuroborreliosis and AD [36]. To evaluate how *B. burgdorferi* bacteria can contribute to the development and/or progression of AD, we studied protein expression of A β aggregates and assessed p-Tau protein tangles before and after infection with *B. burgdorferi* in human cell lines

in vitro using western blot analyses. The tissues were analyzed for the presence of *B. burgdorferi* spirochetes and biofilms using polymerase chain reaction (PCR), fluorescence *in situ* hybridization (FISH), and immunohistochemical methods (IHC). Alginate marker was used to determine biofilm presence. A β and p-Tau specific IHC techniques were utilized for amyloid and p-Tau proteins in tissue slides. Additionally, atomic force microscopy (AFM) enabled us to evaluate the 3-dimensional (3D) morphology of the biofilms in the brain tissues.

MATERIALS AND METHODS

Brain tissue specimens

Formalin fixed paraffin embedded tissue sections of the hippocampus from donors (average age of 75 years) diagnosed with neurodegenerative diseases ($n=10$) including AD ($n=6$), Parkinson's disease ($n=4$), and age-matched non-diseased controls ($n=10$) were obtained from University of Miami via the NIH NeuroBioBank. Archived paraffin-embedded brain autopsy specimens from a patient diagnosed with AD along with sera and PCR positive for *B. burgdorferi* were obtained from McClain Laboratories, LLC (Smithtown, NY). The tissue was fixed and embedded in paraffin blocks, sectioned at 4 microns on TRUBOND200 adhesive slides. The fixed sections of the brain were from the frontal lobe area as well as the hippocampus. Obtaining these human autopsy samples were approved by the University of New Haven Institutional Review Board Committee: exempt under 45 CFR 46.101(b) (4): Research involving the collection or study of existing data, documents, records, pathological specimens, or diagnostic specimens, if these sources are publicly available or if the information is recorded by the investigator in such a manner that subjects cannot be identified, directly or through identifiers linked to the subjects.

Cell culture

Neuroblastoma BE2C cell line (ATCC CRL-2268) was cultured with DMEM media (Sigma Aldrich- D5648) has high glucose containing 1% Penicillin-Streptomycin-Glutamine (PSG) (ThermoFisher Scientific-10378016) and 10% Fetal Bovine Serum (FBS) (ThermoFisher Scientific-21700075) under standard tissue culture conditions. Neuroblastoma Kelly cell line (Sigma-92110411) was grown in

RPMI-1640 media (Sigma-R6504) containing 2 mM glutamine and 10% FBS under standard tissue culture conditions.

Infection with B. burgdorferi

Infection of the human cells with *B. burgdorferi* was conducted based on a previously published protocol [47]. Each cell line was cultured 48 h prior to bacterial infection with respective culturing media supplemented with 10% FBS and 1% PSG. For the *B. burgdorferi* infection, each cell line was cultured to 70% confluency on 60 mm dishes at 37°C and 5% CO₂ in a humidified incubator. 2 × 10⁶ cells *B. burgdorferi* (ATCC 35210, Manassas, VA, USA) were pelleted at 5000 g for 10 min and resuspended in 500 µL of co-culture media composed of the mixture of two-thirds BSK-H medium (Sigma Aldrich, Louis, MO) with 6% rabbit serum and one-third serum and antibiotic free growth media depending on the cell type and added to the cells with MOI 40. After each treatment time, the media were removed from the 60 mm dish and the cells were washed once with PBS. The cells were then pelleted and stored in -80°C freezer.

DNA extraction

For the cell lines used in this study, the extraction of genomic DNA (gDNA) was performed using GeneJET GenomicDNA Purification Kit (ThermoFisher Scientific-K0722). For the tissues, fixed autopsy samples were homogenized by freezing in liquid nitrogen and grinding with a mortar and pestle. The samples were resuspended in 180 µL of Buffer ATL (Qiagen Sciences Inc., Germantown, MD, USA) with 20 µL of Proteinase K (Qiagen), then incubated overnight at 56°C with shaking. DNA was purified by standard phenol/chloroform extraction and alcohol precipitation the following day. Purified DNA was resuspended in 50–100 µL of 1 × TE buffer at pH 8.0 (10 mM Tris, pH 8.0, and 1 mM EDTA).

As a positive control for *B. burgdorferi*, DNA was extracted from a low passage culture of *B. burgdorferi* strain B31 (ATC #35210). Laboratory cultures were maintained in Barbour-Stoner-Kelly-H medium (BSK-H, Sigma), supplemented with 6% rabbit serum (Pel-Freeze Biologicals) and incubated at 33°C with 5% CO₂. The DNA samples were quantified using a BioTek (Winooski, VT, USA) microplate spectrophotometer.

PCR and sequence analysis

B. burgdorferi DNA was detected in the samples using PCR protocols to amplify *Borrelia* 16S ribosomal DNA small subunit or CTP synthase genes as described in previous studies [48]. As negative controls, the same experiments were carried out with *E. coli* DNA as well as a no template DNA. The 16S rDNA gene was amplified in a single reaction using primers F: 5'-CCTGGCTTAGAACTAACG-3'; R: 5'-CCTACAAAGCTTATTCCTCAT-3' in a 50 ml reaction containing HotStarTaq buffer (Qiagen) 1.5 mM MgCl₂, 25 pmoles of each primer, and 2.5 units of HotStarTaq DNA polymerase (Qiagen). Reaction conditions were an initial denaturation at 94°C for 15 min, followed by 40 cycles of 94°C/30 s, 50°C/30 s, 72°C/1 min and a final extension at 72°C/5 min.

CTP synthase sequences were amplified in nested reactions as described previously [48]. First round primers were F: 5'-ATTGCAAGTTCTGAGAATA-3' and R: 5'-CAAACATTACGAGCAAATTC-3' in a 25 ml reaction with HotStarTaq buffer (Qiagen), 25 pmoles of each primer, MgCl₂ adjusted to 2.5 mM, and 1.5 units HotStarTaq. Reaction conditions were an initial denaturation at 94°C for 15 min, followed by 94°C/30 s, a 55°C step down from to 48°C decreasing 1°C per cycle, followed by 30 cycles of 94°C/30 s, 48°C/30 s, 72°C/30 s and a final extension at 72°C/5 min. The nested reaction primers were F: 5'-GATATGGAAAATATTTTATTTATTG-3' and R: 5'-AAACCAAGACAAATTC CAAG-3' in a 50 µL reaction containing 25 pmoles of each primer, 2.5 mM MgCl₂, 1.5 units HotStarTaq. Reaction conditions were an initial denaturation at 94°C for 15 min, followed by 35 cycles of 94°C/30 s, 50°C/30 s, 72°C/30 s and a final extension at 72°C/5 min. The PCR products were visualized by standard agarose gel electrophoresis using SYBR Safe DNA Gel Stain (Invitrogen).

PCR products were purified using the QIAquick PCR purification kit (Qiagen) according to the manufacturer's instructions. Samples were eluted twice in 30 µL, and the eluates from each sample were pooled and sequenced in both directions using the primers that generated the products. Sequencing reactions were performed by Eurofins/MGW/Operon (Huntsville, AL). The sequences obtained were compared to the known sequences in the National Center for Biotechnology Information (NCBI, Bethesda, MD, USA) GenBank database using the Basic Local Alignment Search Tool for nucleic acids (BLASTn).

PCR results were then considered positive if confirmed by sequencing data.

Basic Fuchsin histology

The protocol was based on a previously established histological protocol designed to detect spirochetal organisms [49] with modifications to accommodate microwave-controlled heat delivery to the staining solutions and addition of an aqueous ammonia-based color elution step.

Formalin fixed paraffin embedded tissues are sectioned at three-micron thickness using standard histology technique and heat annealed at 60°C to clean glass slides, followed by wax removal (deceration) in serial xylene and serial alcohol solutions from absolute alcohol to H₂O (90, 80, 70%) terminating in 100% H₂O.

Slides were stained by immersion in a 0.5% Basic Fuchsin solution (Basic Fuchsin powder #CAS632-99-5, Color Index 42510, American Mastertech Scientific Inc., Lodi, CA) in 91% isopropyl alcohol. Basic Fuchsin/alcohol working solution filled single use disposal plastic slide carriers hold a single glass slide. The plastic carrier box is capped and placed inside of a plastic Coplin jar. The Coplin and plastic slide carrier unit is capped and placed inside a microwave oven which is heated at a 30% POWER setting for 1 min. The glass slide is removed and allowed to cool to room temperature and a distilled H₂O wash of the stained slide is completed. The stained slide is then carefully decolorized in a glass Coplin Jar filled with a solution of 30% household ammonia (Household Ammonia Publix Inc, USA) in distilled water. The decolorization progress was monitored visually to detect of loss of red color eluted from the tissue sections and parallel microscopic examination was accomplished of the tissue under 100x magnification to reach a final color differentiation endpoint marked by the appearance of yellow (unstained) color in brain tissues and by detection of persistent red basic fuchsin staining of spirochetes in the tissue. Slides are then washed once in distilled H₂O, air dried, and covered by coverslips. Light microscopy at 400x and 1000x final magnifications was used to identify any red color spirochetes. Photo microscopy through a trinocular head five-megapixel digital camera was completed.

Immunohistochemical analysis

The paraffin-embedded tissue slides were deparaffinized by heating on a slide warmer for 20 min

at 45°C and washing thrice in 100% xylene for 5 min followed by rehydration in series of graded alcohols (100%, 90%, and 70% for 3 min each) and a 30-min rinse under slow-running tap water. Sections were then washed in 1xPBS (pH 7.4) (Sigma) for 5 min followed by distilled water for 5 min. Following deparaffinization and rehydration of the formalin-fixed paraffin-embedded sections, slides were then blocked with a 1 : 100 dilution of goat serum (Thermo Scientific) in 1X PBS (Sigma) for 30 min at room temperature in a humidified chamber. The sections were then washed twice in 1X PBS (Sigma) for 5 min, followed by distilled water for 5 min. Excess solution was gently removed from each slide.

The sections were then incubated overnight with a 1 : 100 dilution (1X PBS/1% BSA) of primary anti-alginate rabbit polyclonal antibody (kindly provided by Dr. Gerald Pier, Harvard Medical School, Boston, MA, USA) at room temperature in a humidified chamber. Sections were then washed as described above and incubated with secondary anti-rabbit antibody with a fluorescent red tag (goat anti-rabbit IgG (H+L)), DyLight 594 conjugated antibody (1 : 200 in 1X PBS pH 7.4, Thermo Scientific), for 1 h in a humidified chamber. Sections were again washed as described above. The slides were then incubated for 1 h with FITC-labeled polyclonal rabbit anti-*Borrelia burgdorferi* at a 1 : 50 dilution (PA-1-73005, Thermo Scientific) in the humidified chamber at room temperature. The sections were washed again as described above counterstained with 0.1% Sudan Black (Sigma) for 20 min, washed and then counterstained with 4', 6-diamidino-2-phenylindole (DAPI, 1 : 1000 in 1X PBS, Thermo Scientific) for 2 min. Finally, the sections were washed and mounted with PermaFlour (Thermo Scientific). Images were captured using a Leica DM2500 fluorescent microscope at 200x and 400x magnification. As negative controls, normal brain sections were stained following the same procedure as mentioned above. Additional negative controls such as omitting the primary antibody and use of non-specific isotype IgG controls (IgG1 Isotype Control, Invitrogen, MA1-10406) were also utilized to confirm the specificity of the antibodies.

Immunohistochemical analysis using A β and phospho-tau markers

Staining for A β proteins and phosphorylated tau was performed on consecutive sections from blocks that were positive for *B. burgdorferi*. Sections were processed and washed as described above, followed

by incubation with a 1 : 200 dilution of either anti- β -amyloid antibody-1 (ABA-1) (MA1-34553, Thermo Fisher Scientific) and secondary anti-rabbit antibody with a fluorescent blue tag (goat anti-rabbit IgG (H+L), DyLight 405 conjugated), following previously published IHC protocols [50]. Alternatively, sections positive for *B. burgdorferi* were incubated with 1 : 200 dilutions of anti-phospho-tau monoclonal antibody (MN1020, Thermo Scientific). As a negative IHC control, a non-specific mouse IgG1 isotype (MA1-10406, Invitrogen) was used in place of the primary antibodies to confirm the antibody specificity of this assay). To avoid any cross-reaction with the different primary and secondary antibodies, sequential sections were used from the same brain section for *Borrelia*, alginate and amyloid staining.

Western blot analyses

Proteins were extracted from infected and non-infected cells using NP-40 lysis buffer (Thermo-Fisher Scientific- J60766-AP), quantified using Biorad Bradford assay (Bio-Rad- 5000006). Proteins were loaded along with the Precision Plus protein ladder (Bio-Rad, #1610376) in 4–15% Mini-PROTEAN TGX Precast PAGE Gel (Bio-Rad, #456–1083) and the gel was run 30 min then transferring the gel using Trans-Blot Turbo, 0.2 μ m PVDF (Bio-Rad, #1704 156EDU) in Trans-Blot Turbo Transfer System for 10 min. For blocking and antibodies, 1% BSA blocking buffer was added and the membranes were kept on shaker at 4°C for 1 h. Membranes were washed 3 times with 1X TBST (Tris-Buffered Saline/Tween 20 Sigma-Aldrich, P1379) for 10 min each. Primary antibodies; GAPDH, Anti-rabbit (1 : 1000, Signalway, #4159-1), Monoclonal Anti-Human Beta-Amyloid antibody (1 : 800, Abcam, ab32136) and Monoclonal Anti-Human Phospho-Tau antibody (1 : 800, ThermoScientific, MN1020) were added and incubated with respective membrane part on shaker at 4°C overnight then each membrane was washed thrice with 1X TBST for 10 min. Human IgG, Anti-rabbit (1 : 1000, Abcam, #ab2075718) secondary antibody was added and incubated on shaker for 1 h at 4°C then the membranes were washed again with 1X TBST thrice each for 10 min. For visualization, ECL Substrate & Peroxidase solution (Bio-Rad, #1705060) were prepared following manufacturer's instructions and each membrane was incubated in the mixture for

5 min then visualized under a chemiluminescence setting in the Gel Documentation System. The percentage of intensity of each band was recorded using ImageJ software (ImageJ.nih.gov, <https://imagej.nih.gov/ij/index.html>) and significance was tested on the average of three experiments using unpaired *t*-test and statistical analysis determined by using the Holm-Sidak method, with $\alpha = 0.05$.

Fluorescent in situ hybridization

FISH was performed on paraffin-embedded human brain tissues using a previously validated protocol [27]. The tissue sections were deparaffinized and rehydrated as stated above. Sections were then placed in a sodium borohydride solution (0.1 μ g in 10 mL, Fisher) for 20 min on ice. The slides were fixed with 4% paraformaldehyde (PFA, J. T Baker) for 15 min at room temperature. The sections were washed in 2X saline sodium citrate (SSC) buffer (3.0 M NaCl, 0.3 M Na Citrate, and dH₂O) and then digested with pre-warmed proteinase K solution (20 μ g/mL in 50 mM Tris, AmericanBio) for 10 min at 37°C. Tissues were then refixed in 4% PFA for 10 min at room temperature.

The slides were then placed into a preheated denaturing solution (70% v/v formamide, 2X SSC, 0.1 mM ethylenediaminetetraacetic acid [EDTA])) and incubated for 5 min at 95°C. The slides were refixed again with 4% PFA for 10 min, washed, and added to denaturing solution again for 2 min at 60°C. The slides were washed in 2X SSC for 5 min at room temperature. Pre-hybridization was followed by incubation for 1–4 h in hybridization buffer (50% v/v formamide, 10% w/v dextran sulfate [Sigma], 1% v/v Triton X-100 [Sigma], 2X SSC, and 2.5 ng of salmon sperm DNA). Hybridization followed by incubating the slides with a denatured 16S rDNA *B. burgdorferi* specific FISH probe (FAM-5'-GGATATAGTTAGAGATAATTATTCCTCCGTTTG-3', Eurofins MWG Operon) at 48°C for 18 h in the dark, A cover slip was placed on each slide to ensure hydration of the tissue throughout the incubation. Post-hybridization, slides were washed twice in 2x SSC at room temperature for 5 min, and then washed in 0.2x SSC for 5 min in the dark. The tissue was then counterstained with 0.1% Sudan Black (Sigma) for 20 min and then washed. Tissues were counterstained with 4',6-diamidino-2-phenylindole (DAPI, Sigma) for 2 min and slides were mounted with Permafluor (Thermo Scientific).

All steps were repeated with several negative controls like 1) 200 ng of unlabeled competing oligonucleotide included during the hybridization (5'-CA AACGGGGAATAATTATCTCTAACTATATCC-3'), 2) following a DNase treatment of the sections before the hybridization step in order to digest all genomic DNA (100 μ g/mL for 60 min at 37°C, and 3) 100 ng negative control random oligonucleotide (FAM-5'-GCATAGCTCTATGACTCTATACTGGTACGTAG-3'). Images were acquired using a Leica DM2500 fluorescent microscope at 200x and 400x magnification.

Confocal microscopy

The tissue sections were visualized and analyzed with a confocal scanning laser microscope (Leica DMI6000) for generating z-axis stacks for visualization of biofilms in a 3-D view. ImageJ software (ImageJ.nih.gov, <https://imagej.nih.gov/ij/index.html>) was used to process the obtained z stacks to provide a detailed analysis of the spatial distribution of the positively stained structure (Plugins: Interactive 3D Surface Plot and Volume Viewer).

Atomic force microscopy

The *Borrelia* alginate-positive structures were visualized at nanometer-scale resolution through AFM analyses. AFM scans on *Borrelia* positive tissues were performed in contact mode using the Nanosurf Easyscan 2 AFM (Nanosurf) equipped with a SHOCONG-10 probe tip (AppNANO, Mountain View, CA, USA). Images were taken by Hamamatsu ORCA Digital Camera. Images were processed using Gwyddion software in order to generate a 3D topographic view of biofilm forms.

RESULTS

One of the main purposes of this study was to evaluate the link between *B. burgdorferi* infected tissues and neurodegenerative diseases. First, we screened brain samples from patients diagnosed with either AD or Parkinson's disease. We then evaluated the presence and morphology of *B. burgdorferi* positive staining from the hippocampal and frontal lobe regions from the same AD/Lyme patient's autopsy tissues.

The status of p-Tau and A β deposits in plaques in *B. burgdorferi* positive tissues and *B. burgdorferi* infected cells were microscopically examined.

IHC staining and PCR analyses of brain autopsy samples for *B. burgdorferi*

In the first set of experiments, the potential presence of *B. burgdorferi* in the brain tissues was investigated. We began by screening 10 brain samples from patients diagnosed with either AD (6) or Parkinson's disease (4). Unfortunately, opportunities to cut additional slides from any tissue in the archived wax blocks from most of these patients were limited because of the depletion of residual tissue by previous investigations. Therefore, the performance of histology studies was, in some experiments, numerically limited by availability of tissue sections. To detect *B. burgdorferi* DNA, a previously published *B. burgdorferi* specific PCR protocol was utilized [47] by the amplification of CTP synthase. A positive band at 650 bp was for two of the AD patient samples and for the isolated *B. burgdorferi* DNA were detected (Fig. 1A). No PCR template negative control (Fig. 1A, lane 3) and none of the normal brain tissues (result not shown) produced detectable PCR bands. Sequencing of the positive PCR products showed 100% identity for *B. burgdorferi* sensu stricto species.

To further confirm the presence of *B. burgdorferi*, we performed fluorescent IHC technique in one of a brain autopsy tissue sample of the PCR positive patient revealed *Borrelia* spirochetes (Fig. 1B). Confocal microscopy analyses clearly showed a *B. burgdorferi* positive spirochetal structure (Fig. 1D).

In our next set of experiments, we further investigated the presence and morphology of *B. burgdorferi* antigen and DNA as well the potential co-localization to amyloid markers. As mentioned above, the tissues from Harvard bank were limited and we needed more materials for a comprehensive study. We were able to study additional autopsy samples from an AD patient who was also diagnosed with Lyme disease by western blot and *Borrelia* DNA presence was reported by a recent study in these brain tissues [36]. The patient's blood and CSF samples were positive for multiple *Borrelia* species [36].

To confirm the presence of *B. burgdorferi* (both sensu stricto and sensu lato species), a PCR was conducted using a previously reported 16S rDNA protocol [47]. The genomic DNA of *Borrelia burgdorferi* B31 laboratory strain was included as a positive control and *E. coli* genomic DNA along with a no DNA template were used as negative controls. Figure 2 demonstrates a positive band for the genomic DNA of the hippocampus region of the patient's brain, indicating the presence of

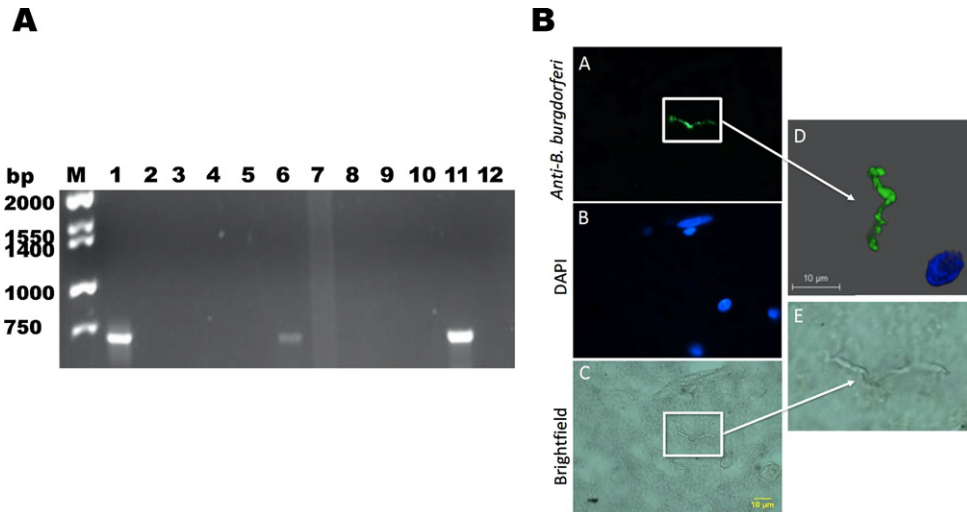


Fig. 1. Analyses of potential presence of *B. burgdorferi* in patients diagnosed with neurodegenerative diseases. A) *B. burgdorferi* specific PCR detection. Bands at 706 bp indicate nested amplification of CTP synthase and the presence of *B. burgdorferi* DNA. A positive control consisting of *B. burgdorferi* B31 gDNA (lane 1) and a negative control with no DNA template were used (lane 2). Positive bands were observed in two AD patients (lane 6 and 11) indicating the presence of *B. burgdorferi* in these brain tissues. B) *B. burgdorferi* spirochete found in brain tissue section of PCR positive patient diagnosed with AD (lane 11). Panel A shows a positively stained *Borrelia* spirochete. D) The morphology of the spirochetal structure seen in panel A which was IHC positive for *B. burgdorferi* was further analyzed by confocal microscopy. Panel E shows the structure stained in panel A and C magnified. Panels A-C were imaged at 1000x magnification.

B. burgdorferi. No PCR products were seen in the no DNA template and the *E. coli* DNA sample, confirming that there was no contamination or nonspecific PCR amplification in the samples. The PCR positive bands were sequenced and compared to known sequences in the NCBI's GenBank database using the Basic Local Alignment Search Tool (BLAST) and the obtained sequence showed 100% identity for *B. burgdorferi* sensu stricto species.

Different forms of *B. burgdorferi* in brain tissues

In the next experiments, we asked the question as to how frequently we can find *B. burgdorferi* positive staining and what kinds of morphological forms are manifest [21–23, 27]. One hundred and fifty tissue slides were obtained from the hippocampal and frontal lobe regions from the same AD/Lyme patient's autopsy tissues. The tissues were stained for *B. burgdorferi* and its biofilm marker, alginate. The IHC staining results showed dominantly *B. burgdorferi* aggregates co-stained with alginate suggesting the presence of true *Borrelia* biofilm form. Out of 150 slides, 100 slides (66%) contained one or two *Borrelia*/alginate positive structures with sizes ranging from 10 to 200 micrometer in diameter. To visualize the spirochetal morphology in the tissues, we adapted a Basic Fuchsin histology staining protocol

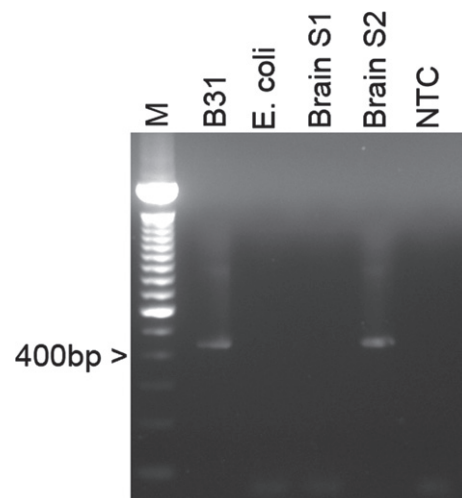


Fig. 2. Representative agarose gel image of a *B. burgdorferi* specific 16S rDNA PCR amplification of genomic DNAs from brain autopsy tissues. Lane 1: 1 kb DNA Ladder (Life Technologies), Lane 2: Extracted genomic DNA from *B. burgdorferi* B31 laboratory strain, Lane 3: Genomic *E. coli* DNA as a negative control, Lanes 4-5: Genomic DNA from human brain autopsy sections from the frontal lobe (S1) and the hypothalamus area (S2), Lane 6: No template control.

which is designed to visualize spirochetal structures [49]. Figure 3 shows representative images of Basic Fuchsin positive structures with evident spirochetal

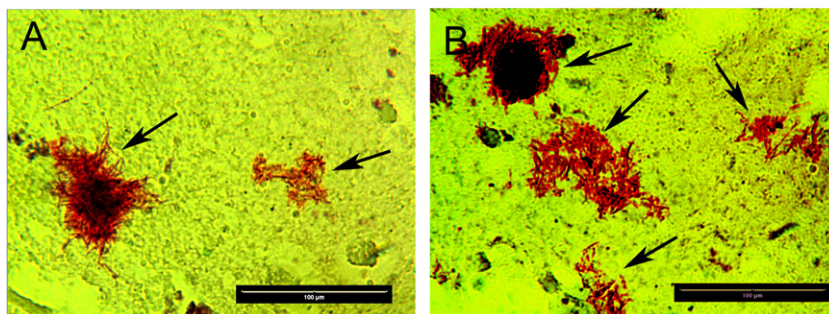


Fig. 3. Representative images of Basic Fuchsin positive structures with evident spirochetal morphology (black arrows, red staining) in autopsy of cerebral cortex from the patient diagnosed with AD and Lyme disease. Magnification 400x, Size bars = 100 microns.

morphology (black arrows, brown staining, Fig. 3A and B). Autopsy cerebral cortex with *Borrelia* in colony growth patterns in closely grouped or in overlapping *Borrelia* (red borrelia against a yellow color brain surround) demonstrates areas of “medusa” pattern *Borrelia* microbes at the edges of the colonies. Absent in these images is any staining of biofilm requisite extracellular matrix which would appear as a “red-veil” of amorphous red staining and would correspond to cell free carbohydrate, protein, and eDNA derived from once living but now dead biofilm microbes. It is possible that the extracellular matrix was completely decolorized from the colonies herein and that only the cell walls of the *Borrelia* retained the Basic Fuchsin stain. Single solitary red color *Borrelia* with a beaded pattern are present in Fig. 3A.

Co-localization of alginate and amyloid markers in B. burgdorferi positive structures

The pathology report of the patient described amyloid plaques in the tissue [36], leading us to assess the possibility of a co-localization of the amyloid proteins with *Borrelia* aggregates in autopsy brain sites. Figure 4 shows images with representative aggregates in the sections of the patient's brain tissues which stained positive for *B. burgdorferi* (green staining, Fig. 4A, E, and I) along with anti-alginate (red staining, Fig. 4B, F, and J) antibodies as well as co-localization with the anti-amyloid protein antibody (blue staining, Fig. 4C, G and K). To avoid any cross-reaction with the different primary and secondary antibodies, sequential sections were used from the same brain section for *B. burgdorferi*, alginate and amyloid staining. Differential interference contrast (DIC) microscopy images help to visualize the tissue structure and biofilm morphology (Fig. 4D, H, and L). As a negative control, only the secondary

antibody without the primary antibody was used. Obtained results showed no positive staining with any of the secondary antibodies (Fig. 4M-O). A DIC microscopy image is included to visualize the part of the brain used in these experiments (Fig. 4P).

The results described above were further assessed for the possibility of co-localization of tau proteins with *Borrelia* positive aggregates due to this protein's association with AD. In additional brain tissue sections from the same AD/Lyme disease patient, *Borrelia*/alginate positive structures were also stained for phospho-tau again in a sequential section to avoid any potential false positive staining. Figure 5 shows that aggregates which stained positive for anti-*Borrelia* (green staining, Fig. 5A), as well as anti-alginate (red staining, Fig. 5B) antibodies, also stained with the anti-phospho-tau antibody (blue staining, Fig. 5C). As a negative control for phospho-tau antibody, a non-specific IgG replaced the primary antibody. Figure 5D shows that there was no staining obtained using only the secondary antibody in this IHC experiments. A DIC image is included to visualize the tissue structure and aggregate morphology (Fig. 5E).

Fluorescence in situ hybridization provide further proof for B. burgdorferi presence in brain tissues

A previously published FISH protocol [23] using *B. burgdorferi* sensu lato specific 16S rDNA probe was utilized to further confirm the presence of *Borrelia* DNA in the brain autopsy tissues (Fig. 6A). DAPI nuclear counterstain was used to depict the nuclear content of the tissue (Fig. 6B) and DIC microscopy was utilized to visualize the morphology of both the aggregates and the host tissue (Fig. 6C). Several negative controls were used to assess the specificity of the

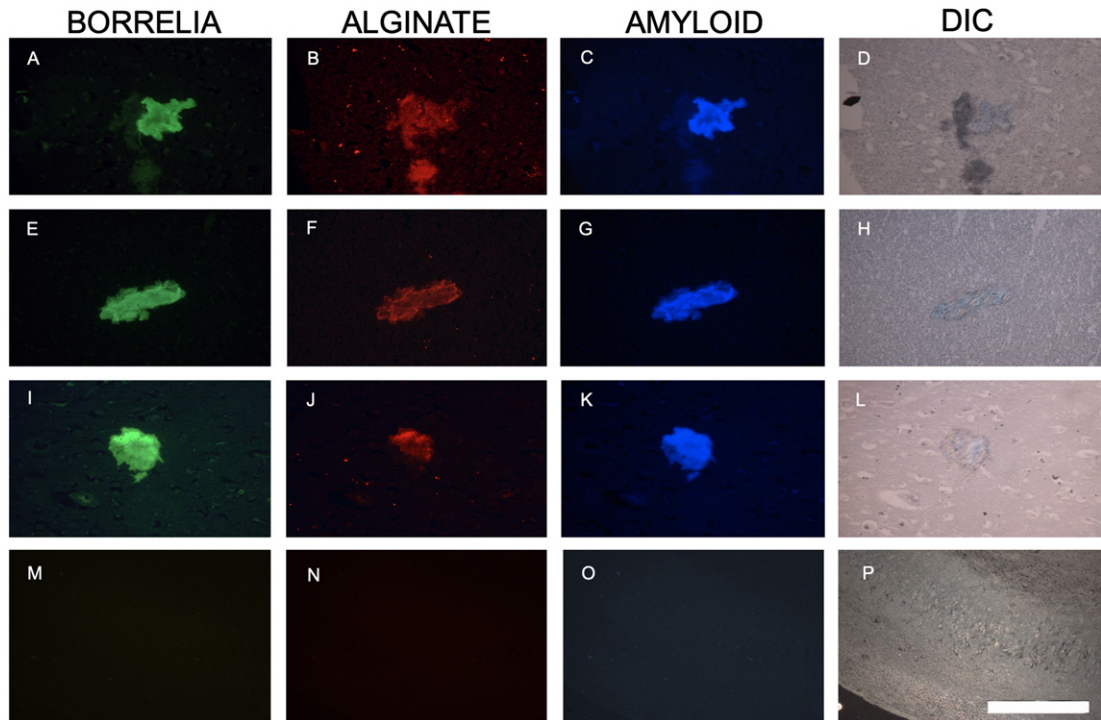


Fig. 4. Representative immunofluorescence images of *B. burgdorferi* positive aggregates with amyloid co-localization in a human brain tissue section. Panels A, E, and I show IHC staining results for infected brain autopsy tissue using a FITC labeled anti-*Borrelia* antibody (green). White arrow shows a *B. burgdorferi* antigen positive spirochete. Panels B, F, and J show results using anti-alginate antibody (red). Panels C, G, and K show results with A β antibody (blue). Panels D, H, L, and P demonstrate tissue morphology with DIC microscopy. Panels N and O show experiments omitting primary antibodies, but secondary antibodies, as negative control. For Panel M, the FITC labeled anti-*Borrelia* antibody, an FITC labeled anti-rabbit antibody was used to mimic the green, fluorescent staining. All images were taken at 400x. The scale bar shows 200 micrometers.

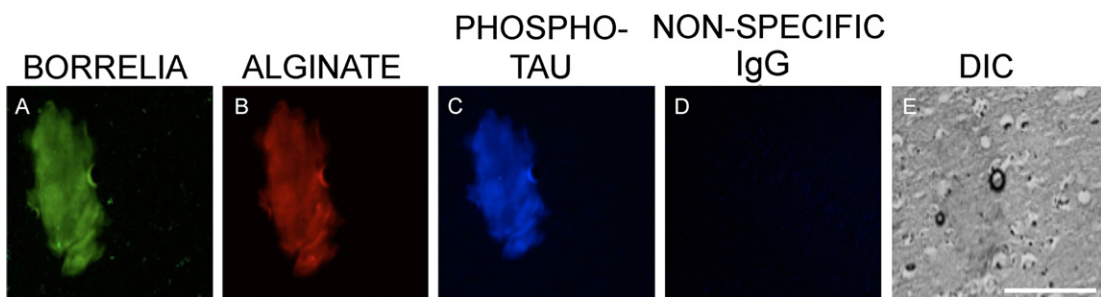


Fig. 5. Representative images of a *B. burgdorferi* positive aggregate with phospho-tau co-localization in human brain tissue sections. Panel A shows IHC staining results for infected brain tissue using a FITC labeled anti-*Borrelia* antibody (green). Panel B shows results using anti-alginate antibody (red). Panel C shows staining with anti-phospho-tau antibody (blue). Panel D demonstrates non-specific IgG negative control and Panel E shows tissue morphology with DIC microscopy. All images were taken at 400x. The scale bar shows 200 micrometers.

FISH probe. The use of a random probe (Fig. 6D), as well as a competing oligo probe (Fig. 6E), and DNase treatment before the *Borrelia* specific probe was added (Fig. 6F), resulted in no visual staining on the sequential sections of the human brain autopsy tissues.

3D demonstration of a *Borrelia*/alginate-positive aggregate by AFM

In the last set of experiments, in order to better understand the detailed structure organization of *Borrelia*/alginate-positive aggregates, contact-mode

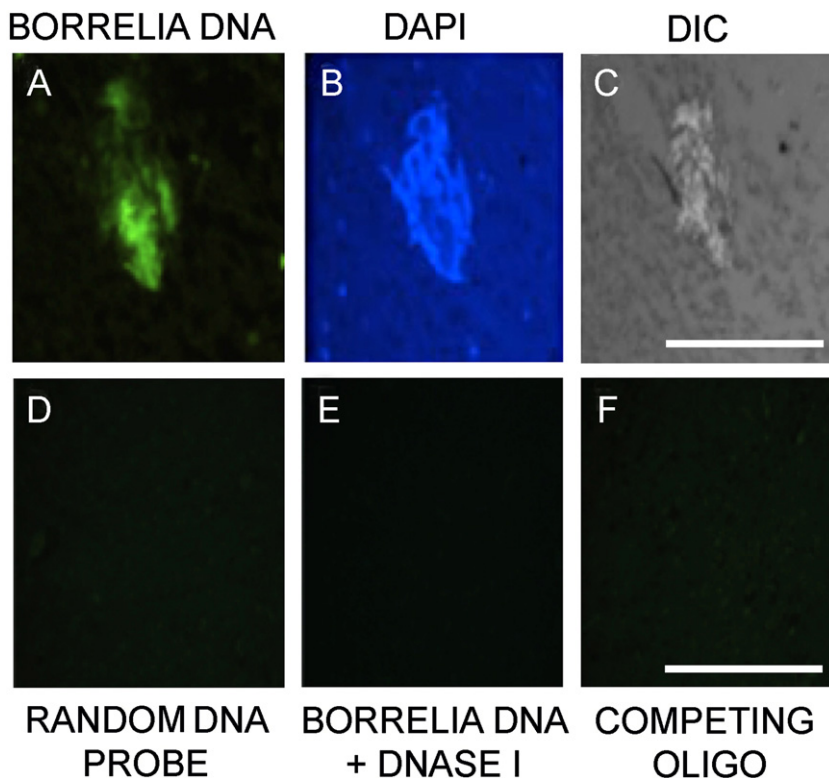


Fig. 6. Fluorescence *in situ* hybridization confirmation of *Borrelia burgdorferi* biofilm-like aggregates in the patient brain tissue. Panel A shows result with *Borrelia* 16s rDNA probe. Panel B shows DAPI nuclear stain. Panel C demonstrates the tissue morphology by DIC microscopy. Panel D shows no staining from an unspecific random DNA probe to further prove the specificity of the *Borrelia* specific DNA probe. Panel E show result of a DNase pretreated tissue section before adding *Borrelia* DNA probe in the experiments. Panel F shows results of a competing oligo+DNA probe. All the images were taken at 400x. The scale bar shows 200 micrometers.

atomic force microscopy was utilized. Figure 7 shows representative micrographs of an IHC stained human brain tissue which was positive for both *Borrelia* and alginate markers. AFM image shows that biofilm was formed by *B. burgdorferi* in closely crowded biofilm configurations in the autopsy tissue and demonstrate the characteristic of empty channels and protrusions with “tower morphology” as previously demonstrated in *Borrelial* lymphocytoma human biopsy tissues [23]. Round body *Borrelia* AFM profiles have been previously published [23] from *Borrelia garinii* species in biofilm communities. The patient presented here had AD and tested positive for triple *Borrelia* species (*Borrelia garinii*, *Borrelia afzelii*, and *Borrelia burgdorferi*) by western blot studies several times during life [36]. Round body profiles of specialized non-motile *Borrelia* inside the biofilm community distinguish biofilm *specialized* type round body *Borrelia* from their motile cylindrical planktonic precursors.

A β and p-Tau status in *B. burgdorferi* infected cells

The above-mentioned results strongly suggest a causal relationship between *B. burgdorferi* infection and amyloid and p-Tau productions. To further evaluate whether *B. burgdorferi* could contribute to p-Tau and A β aggregation, we infected neuroblastoma cells with *B. burgdorferi* using previously established protocol [50]. To provide evidence that the infected cells indeed have *B. burgdorferi*, a 16S rDNA specific PCR protocol was utilized [47]. Supplementary Figures 1 and 2 show that as early as 24-h post-infection, *B. burgdorferi* is present in both cell lines and even at 72 h is still detectable.

To evaluate whether *B. burgdorferi* infection might contribute to increased level of A β and p-Tau, western blot assay was performed and the level of both proteins before and after infection was analyzed. Both A β and p-Tau proteins have shown a significant increase in protein expression in infected cells

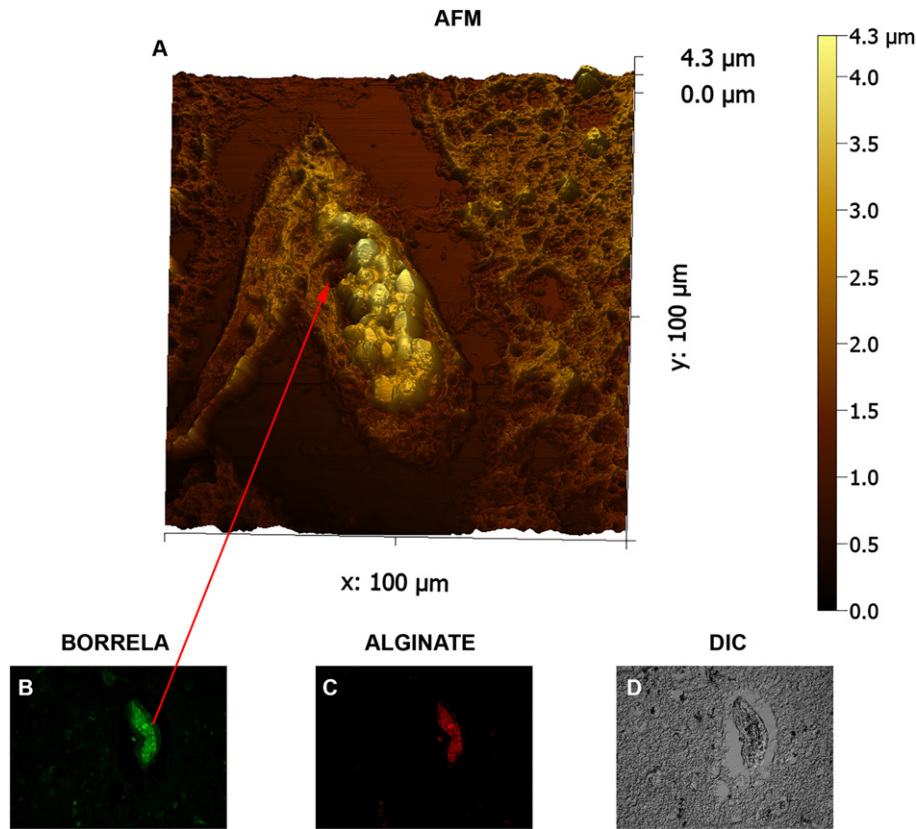


Fig. 7. Three-dimensional atomic force microscopy analyses of *Borrelia*/alginate-positive aggregates from a human brain tissue section. Panel A shows a representative image from the AFM analyses which was performed using contact mode of the Nanosurf Easyscan 2 AFM with SHOCONG probe (AppNANOTM). Images were processed, and measurements were obtained using Gwyddion software. The individual height and width ranges are indicated on the panels. Panel B and C shows evidence that the scanned tissue is *Borrelia*- and alginate-positive by fluorescent IHC analyses (400x magnification). Panel D shows DIC imaging to visualize the tissue. Red arrows represent the same area of the tissue illustrated on panel A. Panel D shows tissue morphology with DIC microscopy. Scale bar: 100 μ m

	Kelly		BE2C		
	+	-	+	-	
<i>B. burgdorferi</i>	+	-	+	-	
Amyloid-Beta					95 KDa
Phospho-Tau					64 KDa
GAPDH					37 KDa

Fig. 8. Expression of A β and p-Tau proteins in infected and non-infected cells. Western blot analysis of protein expression of A β (95 KDa), p-Tau (64 KDa), and GAPDH (37 KDa) of the 48 h of *B. burgdorferi* infected and uninfected Kelly and BE2C cell lines.

compared to uninfected ones (Fig. 8). Intensity and normalization of each band was then analyzed and the statistical analysis of unpaired *t*-test detailed significance between non-infected and infected cells in A β and p-Tau protein expression with $p < 0.05$.

DISCUSSION

This study contributes to the growing number of evidence that chronic infection can play a significant role in the etiology of some diseases such as neurodegeneration. There were several earlier studies that indicated the potential presence of spirochetal organism in brains with degenerative disorders [28–36], and while some studies suggested a potential link [35, 51], others contradicted these findings [52]. In this study, the result of screening human brain tissue sections of patients diagnosed with AD and Parkinson's disease were reported. PCR and histochemical and immunostaining results provided strong evidence for the presence of the Lyme disease causing bacteria, *B. burgdorferi*, in sections of two out of ten patients' brain hippocampus region. Since we had limited tissue sections from these NIH NeuroBioBank samples, we continued our study in more

detail with autopsy tissue sections from a Lyme disease patient with autopsy AD neuropathology confirmation. The autopsy tissue obtained from this patient were analyzed for *B. burgdorferi*, biofilm, and amyloid markers.

B. burgdorferi is known to be capable of forming biofilms *in vitro* and *in vivo* [21–23, 27]. Formation of biofilm communities is distinguished by the emergence of specialized bacterial forms that possess specialized biological behaviors which are not planktonic. A sequence of different physical and physiological properties leads to bacterial resistance to anti-microbial agents which permits for chronic infections to be established [53]. Other microbial biofilms have previously been associated with antibiotic resistance leading to human diseases like cystic fibrosis and native valve endocarditis [54]. Amyloid structures were recently suggested as functional components of bacterial biofilm for both Gram negative and positive bacteria [55, 56].

In our previous study using *Borrelia* infected skin tissues, we provided evidence for the co-localization of *Borrelia* biofilm and amyloid markers [57]. In this study, IHC results showed evidence for both spirochete and biofilm forms in Lyme disease patient with AD pathology with co-localization with the anti-A β antibody, indicating the presence of *Borrelia* around the plaques. Several previous studies provided strong evidence that bacterial amyloid is an important component to in senile plaques in AD by demonstration of co-localization of *Borrelia* antigens and DNA with A β deposits in the brains of those patients [9, 14, 15, 18, 28–36]. Furthermore, increased levels of amyloid- β protein precursor (A β PP) were found in cells that had been infected with spirochete [32]. Additionally, Allen et al. have suggested that AD senile plaques evidently have characteristics of spirochetes and co-localize with A β , strengthening the idea that A β PP is important in both the spirochete and AD plaques [35]. These findings suggest that by exposure to bacteria or the toxic products released by the bacterial spherical bodies such as outer membrane vesicles, can elicit host responses comparable to those observed in many neurodegenerative diseases such as AD [31–33]. AD has not only been associated with *B. burgdorferi* brain infections. As mentioned above, association between AD and infectious agents such as *Chlamydia pneumonia*, *Helicobacter pylori*, *Porphyromonas gingivalis*, and *Propionibacterium acnes* have also been established [37–45]. Amyloid deposition has been associated with chronic human bacterial infections and development of biofilm [58].

The amyloid curli protein can irreversibly form conjugated fibers with bacterial DNA during biofilm formation, which leads to amyloid polymerization and an activated immune response [59]. In this study, it was hypothesized that these biofilm formations of *B. burgdorferi* are detectable in brain tissues with amyloid coated plaques. Co-localization of these *B. burgdorferi* positive aggregates with the alginate deposits verified that there are true biofilm structures. Alginate has also been shown to be the major component of the *Pseudomonas aeruginosa* biofilm in chronic cystic fibrosis and a crucial component of the EPS layer in *B. burgdorferi*, supporting our data of alginate production in *Borrelia* biofilms [21–23, 27, 60].

Clinical research with AD-associated biomarkers for several phosphorylated tau protein classes in autopsy brain pathology immunohistochemical studies discloses high level of phospho-tau proteins in AD compared to controls. This study also included the phospho-tau antibody in the IHC experiments in order to assess possible co-localization of this protein with the *Borrelia* aggregates. In addition to the co-localization of A β with *Borrelia* and alginate, phospho-tau was also found to be co-localized in the tissues. To better visualize and further confirm the presence of *Borrelia* positive aggregates, we applied our sensitive FISH protocol using a *B. burgdorferi* specific 16S rDNA probe. For confirmation of the results, several independent negative controls for the FISH and IHC experiments were incorporated. Negative controls included: IHC experiments with alginate and *Borrelia* performed on the sequential human brain slides, a no- primary or non-specific antibody control incorporated into the IHC experiments, and several FISH negative controls (DNase-treated samples, random DNA probes, and competing oligonucleotide). Additional negative controls were performed on normal human brain tissues. The negative results of these controls verify that the antibodies and probes were specific, and no background tissue staining was detected. This study also provides AFM imaging of the *Borrelia*-positive biofilms in the brain tissues. These nanoscale images allowed us to visualize some detail feature of biofilms 3-dimensional morphology and further characterize the structure of the *Borrelia*- and alginate-positive aggregates showing the classical tower morphology.

Our *in vitro* experiments also suggested that *B. burgdorferi* spirochetes in tissue co-cultures can be associated with the increase deposition of A β . We observed a significant increased expression in the

p-Tau and A β proteins in *B. burgdorferi* infected cells compared to non-infected ones which strongly suggest a functional relationship; however, further larger studies are required to provide explanations of the role of *B. burgdorferi* infection in AD brain.

Bacterial infection is expected to trigger host innate immune response to prevent the spread and movement of pathogens. Upon *B. burgdorferi* invasion, astrocytes and neurons in the spinal cord and brain are known to release signaling molecules such as IL-6, IL-8, IL-10, interferon (IFN)-gamma, and tumor necrosis factor (TNF)-alpha, inducing inflammation seen in acute LNB [61, 62]. This can be followed by infiltration of microglia, macrophages, and T cells to the site leading to higher level of inflammatory mediators and ultimate neuronal apoptosis [61, 62]. In our previous study, we have provided evidence that *Borrelia* biofilm can be surrounded by infiltrating T cells in human autopsy tissues [27]. In one of our recent papers, we have shown that *B. burgdorferi* can increase MCP-1 and MCP-2 cytokine secretion as well as manipulate oxidative stress by downregulating superoxide dismutase 2 (SOD2) gene in BE2C cells [47].

In summary, chronic bacterial infections are among potential important risk factors for neurodegenerative diseases, including AD. In this study, we demonstrated co-localization of *B. burgdorferi* biofilm and amyloid markers and provided evidence that *Borrelia* infection can increase amyloid markers in human cells. However, one of the limitations of this research, that we had limited number of tissues from those neurodegenerative samples and most of the tissues had just a few sections available, therefore we were only able to do more comprehensive study with one *B. burgdorferi* positive sample. We are in the process to reach out to other tissues banks and extend this study with a larger numbers and more significant amounts of brain tissues.

This research is part of a larger body of work that hypothesizes “*chronic infection and it's adaptive pathological consequences can play a key role in the etiology of many diseases such dementia and neurodegeneration*”.

ACKNOWLEDGMENTS

The authors thank the Dr. Paul H. Duray Foundation, Lyme Warriors, University of New Haven URS/SRG/RG, Reinier Elias Stichting, and National Philanthropic Trust for their support. Microscopes

and cameras were donated by Lymedisease.org, the Schwartz Research Foundation and the Global Lyme Alliance. We also thank Dr. Akiko Nishiyama (University of Connecticut) for the use of a Leica SP8 confocal microscope (NIH Shared and High Instrumentation Award #S100D016435). We are also grateful to Minnie Elias-van der lande for her contribution to this research.

Authors' disclosures available online (<https://www.j-alz.com/manuscript-disclosures/21-5398r1>).

SUPPLEMENTARY MATERIAL

The supplementary material is available in the electronic version of this article: <https://dx.doi.org/10.3233/JAD-215398>.

REFERENCES

- [1] Burgdorfer W, Barbour AG, Hayes SF, Benach JL, Grunwaldt E, Davis JP (1982) Lyme disease—a tick-borne spirochetosis? *Science* **216**, 1317-1319.
- [2] Lane RS, Piesman J, Burgdorfer W (1991) Lyme borreliosis: Relation of its causative agent to its vector and hosts in North America and Europe. *Annu Rev Entomol* **36**, 587-609.
- [3] Rodino KG, Theel ES, Pritt BS (2020) Tick-borne diseases in the United States. *Clin Chem* **66**, 537-548.
- [4] Pachner AR (1989) Neurologic manifestations of Lyme disease, the new “great imitator”. *Infect Dis* **11**, 1482-1486.
- [5] Rupprecht TA, Koedel U, Fingerle V, Pfister H-W (2008) The pathogenesis of lyme neuroborreliosis: From infection to inflammation. *Mol Med* **14**, 205-212.
- [6] Bransfield RC (2018) Neuropsychiatric Lyme Borreliosis: An overview with a focus on a specialty psychiatrist's clinical practice. *Healthcare (Basel)* **6**, 104.
- [7] Steere AC, Bartenhagen Nh, Carft JE, Hutchinson GJ, Newman JH, Pachner AR, Rahn DW, Sigal LH, Taylor E, Malawista SE (1986) Clinical manifestations of Lyme disease. *Zentralbl Bakteriol Mikrobiol Hyg A* **263**, 201-205.
- [8] Rebman AW, Aucott JN (2020) Post-treatment Lyme disease as a model for persistent symptoms in Lyme disease. *Front Med* **7**, 57.
- [9] MacDonald AB (1986) *Borrelia* in the brains of patients dying with dementia. *JAMA* **256**, 2195-2196.
- [10] Pennekamp A, Jaques M (1997) Chronic neuroborreliosis with gait ataxia and cognitive disorders. *Praxis* **86**, 867-869.
- [11] Fallon BA, Nields (1994) Lyme disease: A neuropsychiatric illness. *Am J Psychiatry* **151**, 1571-1583.
- [12] Miklossy J, Khalili K, Gern L, Ericson RL, Darekar P, Bolle L, Hurlimann J, Paster BJ (2004) *Borrelia burgdorferi* persists in the brain in chronic lyme neuroborreliosis and may be associated with Alzheimer disease. *J Alzheimers Dis* **6**, 39-49.
- [13] Meer-Scherrer L, Lao CC, Adelson ME, Mordechai E, Lobrinus JA, Fallon BA, Tilton RC (2006) Lyme disease associated with Alzheimer's disease. *Curr Microbiol* **52**, 330-332.
- [14] Miklossy J (2008) Biology and neuropathology of dementia in syphilis and Lyme disease. *Handb Clin Neurol* **89**, 825-44.

- [15] Blanc F, Philippi N, Cretin B, Kleitz C, Berly L, Jung B, Kremer S, Namer IJ, Sellal F, Jaulhac B, de Seze J (2014) Lyme neuroborreliosis and dementia. *J Alzheimers Dis* **41**, 1087-1093.
- [16] Hampf EG (1951) Further studies on the significance of spirochetal granules. *J Bacteriol* **62**, 347-349.
- [17] Brorson O, Brorson SH (1997) Transformation of cystic forms of *Borrelia burgdorferi* to normal, mobile spirochetes. *Infection* **25**, 240-246.
- [18] MacDonald AB (2006) Spirochetal cyst forms in neurodegenerative disorders,... hiding in plain sight. *Med Hypotheses* **67**, 819-832.
- [19] Gruntar I, Malovrh T, Murgia R, Cinco M (2001) Conversion of *Borrelia garinii* cystic forms to motile spirochetes *in vivo*. *APMIS* **109**, 383-388.
- [20] Murgia R, Cinco M (2004) Induction of cystic forms by different stress conditions in *Borrelia burgdorferi*. *APMIS* **112**, 57-62.
- [21] Sapi E, Bastian SL, Mpooy CM, Scott S, Rattelle A, Pabbati N, Poruri A, Burugu D, Theophilus PAS, Pham TV, Datar A, Dhaliwala NK, MacDonald AB, Rossi MJ, Sinha SK, Luecke DF (2012) Characterization of biofilm formation by *Borrelia burgdorferi* *in vitro*. *PLoS One* **7**, e48277.
- [22] Timmaraju AV, Theophilus PAS, Balasubramanian K, Shakih S, Luecke DF, Sapi E (2015) Biofilm formation by *Borrelia sensu lato*. *FEMS Microbiol Lett* **362**, fmv120.
- [23] Sapi E, Balasubramanian K, Poruri A, Maghsoudlou JS, Socarras KM, Timmaraju AV, Filush KR, Gupta K, Shaikh S, Theophilus PAS, Luecke DF, MacDonald AB, Zelger B (2016) Evidence of *in vivo* existence of *Borrelia* biofilm in borrelial lymphocytomas. *Eur J Microbiol Immunol* **6**, 9-24.
- [24] Costerton JW, Stewart PS, Greenberg EP (1999) Bacterial biofilms: A common cause of persistent infections. *Science* **284**, 1318-1322.
- [25] Sapi E, Kaur N, Anyanwu S, Leucke DF, Datar A, Patel S, Rossi MJ, Stricker R (2011) Evaluation of *in-vitro* antibiotic susceptibility of different morphological forms of *Borrelia burgdorferi*. *Infect Drug Resist* **4**, 97-113.
- [26] Feng J, Li T, Yuan Y, Yee R, Zhang Y (2019) Biofilm/persister/stationary phase bacteria cause more severe disease than log phase bacteria—Biofilm *Borrelia burgdorferi* not only display more tolerance to Lyme antibiotics but also cause more severe pathology in a mouse arthritis model: Implications for understanding persistence, PTLDS and treatment failure. *Discov Med* **148**, 125-138.
- [27] Sapi E, Kasliwala RS, Ismail H, Torres JP, Oldakowski M, Markland S, Gaur G, Melillo A, Eisendle K, Liegner KB, Libien J, Goldman JE (2019) The long-term persistence of *Borrelia burgdorferi* antigens and DNA in the tissues of a patient with Lyme disease. *Antibiotics (Basel)* **8**, 183.
- [28] MacDonald AB, Miranda JM (1987) Concurrent neocortical borreliosis and Alzheimer's disease. *Hum Pathol* **18**, 759-761.
- [29] Miklosy J (1993) Alzheimer's disease—a spirochetosis? *Neuroreport* **4**, 841-848.
- [30] MacDonald AB (2006) Plaques of Alzheimer's disease originate from cysts of *Borrelia burgdorferi*, the Lyme disease spirochete. *Med Hypotheses* **67**, 592-600.
- [31] Miklosy J, Kis A, Radenovic A, Miller L, Forro L, Martins R, Reiss K, Darbinian N, Darekar P, Mihaly L, Khalili K (2006) Beta-amyloid deposition and Alzheimer's type changes induced by *Borrelia* spirochetes. *Neurobiol Aging* **27**, 228-236.
- [32] Miklosy J (2016) Bacterial amyloid and DNA are important constituents of senile plaques: Further evidence of the spirochetal and biofilm nature of senile plaques. *J Alzheimers Dis* **53**, 1459-1473.
- [33] Miklosy J (2011) Alzheimer's disease – a neurospirochetosis. Analysis of the evidence following Koch's and Hill's criteria. *J Neuroinflammation*, **8**, 90.
- [34] Kristoferitsch W, Aboulenein-Djamshidian F, Jecel J, Rauschka H, Rainer M, Stanek G, Fischer P (2018) Secondary dementia due to Lyme neuroborreliosis. *Wien Klin Wochenschr* **130**, 468-478.
- [35] Allen HB (2016) Alzheimer's disease: Assessing the role of spirochetes, biofilms, the immune system, and amyloid- β with regard to potential treatment and prevention. *J Alzheimers Dis* **53**, 1271-1276.
- [36] MacDonald AB (2021) *Borrelia* invasion of brain pyramidal neurons and biofilm *Borrelia* plaques in neuroborreliosis dementia with Alzheimer's phenotype. *Microbiol Infect Dis* **5**, 1-11.
- [37] Readhead B, Haure-Mirande JV, Funk CC, Richards MA, Shannon P, Haroutunian V, Sano M, Liang WS, Beckmann ND, Price ND, Reiman EM, Schadt EE, Ehrlich ME, Gandy S, Dudley JT (2018) Multiscale analysis of independent Alzheimer's cohorts finds disruption of molecular, genetic, and clinical networks by Human Herpesvirus. *Neuron* **99**, 64-82.
- [38] Balin BJ, Gerard HC, Arking EJ, Appelt DM, Branigan PJ, Abrams JT, Whittum-Hudson JA, Hudson (1998) Identification and localization of *Chlamydia pneumoniae* in the Alzheimer's brain. *Med Microbiol Immunol* **187**, 23-42.
- [39] Balin BJ, Little Cs, Hammond CJ, Appelt DM, Whittum-Hudson JA, Gerard HC, Hudson AP (2008) *Chlamydia pneumoniae* and the etiology of late-onset Alzheimer's disease. *J Alzheimers Dis* **13**, 371-380.
- [40] Balin BJ, Hammond CJ, Little CS, Hingley ST, Al-Atrache Z, Appelt DM, Whittum-Hudson JA, Hudson AP (2018) *Chlamydia pneumoniae*: An etiologic agent for late-onset dementia. *Front Aging Neurosci* **10**, 302.
- [41] Poole S, Singhrao SK, Kesavalu L, Curtis MA, Crean S (2013) Determining the presence of periodontopathic virulence factors in short-term postmortem Alzheimer's disease brain tissue. *J Alzheimers Dis* **36**, 665-677.
- [42] Poole S, Singhrao SK, Chukkapalli S, Rivera M, Velsko I, Kesavalu L, Crean S (2015) Active invasion of *Porphyromonas gingivalis* and infection-induced complement activation in ApoE-/- mice brains. *J Alzheimers Dis* **43**, 67-80.
- [43] Singhrao SK, Olsen I (2019) Assessing the role of *Porphyromonas gingivalis* in periodontitis to determine a causative relationship with Alzheimer's disease. *J Oral Microbiol* **11**, 1563405.
- [44] Kornhuber HH (1996) Propionibacterium acnes in the cortex of patients with Alzheimer's disease. *Eur Arch Psychiatry Clin Neurosci* **246**, 108-109.
- [45] Kountouras J, Tsolaki M, Gavalas E, Boziki M, Zavos C, Karatzoglou P, Chatzopoulos D, Venizelos I (2006) Relationship between *Helicobacter pylori* infection and Alzheimer disease. *Neurology* **66**, 938-940.
- [46] Knopman DS, Amieva H, Petersen RC, Chetelat G, Holtzman DM, Bradley TH, Nixon RA, Jones DT (2021) Alzheimer disease. *Nat Rev Dis Primers* **7**, 33.
- [47] Wawrzyniak K, Gaur G, Sapi E, Senejani AG (2020) Effect of *Borrelia burgdorferi* outer membrane vesicles on host oxidative stress response. *Antibiotics (Basel)* **9**, 5.
- [48] Sapi E, Pabbati N, Datar A, Davies EM, Rattelle A, Kuo BA (2013) Improved culture conditions for the growth and

- detection of *Borrelia* from human serum. *Int J Med Sci* **10**, 362-376.
- [49] Levine BS (1952) Staining *Treponema pallidum* and other treponemata. *Public Health Rep* **67**, 253-257.
- [50] Miklossy J, Taddei K, Martins R, Escher G, Krafsik R, Pillevuit O, Lepori D, Campiche M (1999) Alzheimer disease: Curly fibers and tangles in organs other than brain. *J Neuropathol Exp Neurol* **58**, 803-814.
- [51] Herrera-Landero A, Amaya-Sánchez, LE, d'Hyver de las-Deses C, Soloranzo-Santos F, Gordillo-Perez MG (2019) *Borrelia burgdorferi* as a risk factor for Alzheimer's dementia and mild cognitive impairment. *Eur Geriatr Med* **10**, 493-500.
- [52] O'Day DH, Catalano A (2014) A lack of correlation between the incidence of Lyme disease and deaths due to Alzheimer's disease. *J Alzheimers Dis* **42**, 115-118.
- [53] Li XH, Lee JH (2017) Antibiofilm agents: A new perspective for antimicrobial strategy. *J Microbiol* **55**, 753-766.
- [54] Donlan RM, Costerton JW (2002) Biofilms: Survival mechanisms of clinically relevant microorganisms. *Clin Microbiol Rev* **15**, 167-193.
- [55] Taglialegna A, Lasa I, Valle J (2016) Amyloid structures as biofilm matrix scaffolds. *J Bacteriol* **198**, 2579-2588.
- [56] Erskine E, MacPhee CE, Stanley-Wall NR (2018) Functional amyloid and other protein fibers in the biofilm matrix. *J Mol Biol* **430**, 3642-3656.
- [57] Middelveen MJ, Filush KR, Bandoski C, Kasliwala RS, Melillo A, Stricker RB, Sapi E (2019) Mixed *Borrelia burgdorferi* and *Helicobacter pylori* biofilms in Morgellons disease dermatological specimens. *Healthcare (Basel)* **7**, 70.
- [58] Romero D, Aguilar C, Losick R, Kolter R (2010) Amyloid fibers provide structural integrity to *Bacillus subtilis* biofilms. *Proc Natl Acad Sci U S A* **107**, 2230-2234.
- [59] Gallo PM, Rapsinski GJ, Wilson RP, Oppong GO, Sriram U, Goulian M, Buttaro B, Caricchio R, Gallucci S, Tükel Ç (2015) Amyloid-DNA composites of bacterial biofilms stimulate autoimmunity. *Immunity* **42**, 1171-1184.
- [60] Høiby N, Ciofu O, Bjarnsholt T (2010) *Pseudomonas aeruginosa* biofilms in cystic fibrosis. *Future Microbiol* **5**, 1663-1674.
- [61] Sjöwall J, Carlsson A, Vaarala O, Bergström S, Ernerudh J, Forsberg P, Ekerfelt C (2005) Innate immune responses in Lyme borreliosis: Enhanced tumour necrosis factor- α and interleukin-12 in asymptomatic individuals in response to live spirochetes. *Clin Exp Immunol* **141**, 89-98.
- [62] Ramesh G, Borda JT, Gill A, Ribka EP, Morici LA, Mottram P, Martin DS, Jacobs MB, Didier PJ, Philipp MT (2009) Possible role of glial cells in the onset and progression of Lyme neuroborreliosis. *J Neuroinflammation* **6**, 23.